

PAPER

Outlier detection of monitored data and unsupervised recognition of construction activities during seismic performance enhancement of historic stone monuments

To cite this article: Songtao Xue *et al* 2025 *Eng. Res. Express* 7 015116

View the [article online](#) for updates and enhancements.

You may also like

- [Localism in perceiving the problem of adat people in forest area: A critical thinking](#)
Agung Wibowo
- [Criterion of Authenticity or New Creation in Historical Fortresses on the Territory of Poland](#)
Ewa Weclawowicz-Gyurkovich
- [Brain-based learning and perception of students in a suburban area about the history](#)
W I Fauzi, A B Santosa and Tarunasena

Engineering Research Express



PAPER

Outlier detection of monitored data and unsupervised recognition of construction activities during seismic performance enhancement of historic stone monuments

RECEIVED
9 October 2024

REVISED
13 January 2025

ACCEPTED FOR PUBLICATION
22 January 2025

PUBLISHED
5 February 2025

Songtao Xue^{1,2,3} , Qinshao Shi¹ , Liyu Xie^{1,3} , Shuning Zhou⁴, Wensheng Lu¹ and Mansheng Zhang⁵

¹ Department of Disaster Mitigation for Structures, Tongji University, Shanghai, People's Republic of China

² Department of Architecture, Tohoku Institute of Technology, Sendai, Japan

³ State Key Laboratory of Disaster Reduction in Civil Engineering, People's Republic of China

⁴ Xi'an Beilin Museum, Xi'an, People's Republic of China

⁵ China Aviation Planning and Design Institute Co. Ltd, Beijing, People's Republic of China

E-mail: liyuxie@tongji.edu.cn

Keywords: cultural heritage preservation, structural health monitoring, structural vibration isolation, internet of things (IoT) monitoring system, unsupervised learning

Abstract

To enhance the seismic resilience of historical and cultural heritage sites, protective measures were implemented through the installation of advanced heritage protection platform facilities. A structural health monitoring system was developed to safeguard historical relics during construction activities by continuously monitoring the overall condition of the relics and the integrity of critical components. Key parameters, such as settlement differences, tilt, crack width, and acceleration, were meticulously tracked, with predefined warning and alarm thresholds established. Alerts were triggered whenever these parameters exceeded their respective thresholds, ensuring timely interventions. To ensure the reliability and consistency of the collected data, this study proposes an evaluation method that integrates multi-source data fusion with statistical analysis techniques. Building on this foundation, an unsupervised algorithm was employed to identify construction activities impacting the structural health of the relics. The results demonstrate the effectiveness of combining multi-source data and intelligent algorithms for reliable monitoring and early detection of risks during conservation. The developed system offers automated, real-time assessments and can serve as a model for future heritage protection projects. Looking forward, integrating wireless sensors and diverse data sources could improve system accuracy, efficiency, and cost-effectiveness, further enhancing the protection of cultural heritage.

Introduction

The conservation of cultural relics not only exemplifies reverence for and the preservation of historical culture but also contributes positively to both social stability and economic development [1–3]. Monuments, as distinctive cultural relics, serve to commemorate and document significant historical events, figures, or societal cultures [4–7].

However, due to the absence of seismic measures and prolonged natural weathering, cultural relics exhibit low resistance to seismic risks. Historical examples demonstrate the vulnerability of historical relics to seismic damage [8–10]. On February 6, 2023, Gaziantep Castle, a UNESCO World Cultural Heritage site, collapsed during the magnitude 7.8 Richter scale earthquake in Turkey. Moreover, the Ministry of Culture and Tourism has identified over 8,000 historic structures in eleven provinces severely affected by earthquakes [11]. Similarly, during the Ming Dynasty, a suspected moment magnitude (Mw) 8 earthquake in Shaanxi, China, caused the collapse or fracture of 40 out of 114 stone monuments, some of which are examined in this paper [12]. These examples highlight the urgent need to enhance the seismic resilience of cultural relics [13].



Figure 1. Frontal perspective of the exhibition room prior to seismic performance enhancement.

In contemporary engineering, two widely adopted methods for improving the seismic resistance of cultural relics are direct fixation to an external frame and the installation of isolation platforms [13, 14]. In contrast to smaller artifacts typically showcased in compact display units, monuments with larger dimension are structurally connected to their bases through foundations. Research indicates that monuments fortified using the two aforementioned methods exhibit resilience against seismic forces, maintaining their upright position during such events [15]. However, employing the direct fixation of the monument to the external frame may result in some cracking in the connection region between the monument and its base. In contrast, the base isolation reinforcement method enhances the monument's direct seismic resistance by extending the vibration period of the entire system, preventing the occurrence of cracks in the connection area between the monument body and its base. Therefore, the installation of isolation platforms for monuments emerges as an effective approach.

This paper focuses on monitoring efforts undertaken during the seismic functional upgrading of an exhibition room in a historic stone monuments museum located in Xi'an, China. As the ancient capital of China during the 13th Dynasty, Xi'an boasts a profound cultural heritage and a rich historical legacy. The museum, with nearly a millennium of existence, houses a significant collection of stone monuments with great artistic value. However, situated at 108.95 °E longitude and 34.27 °N latitude, Xi'an is positioned between the two largest seismic zones globally: the Mediterranean Himalayan Seismic Belt and the Circum-Pacific Seismic Belt. Additionally, it is on the edge of the Qinling Seismic Belt, posing unfavorable conditions for the protection of cultural relics.

In specific terms, each monument involved in the seismic performance enhancement has approximate dimensions of 2 m in height and 1 meter in length, with six monuments forming a group. Several groups of monuments are interconnected by concrete frameworks, forming an elongated concrete structure, as illustrated in figure 1. Unlike smaller relics like statues, these tall and slender monument monuments cannot be directly hoisted for enhancement with relocation. The enhancement process involves cutting the existing foundations, installing steel beams, and using hydraulic jacks to lift the monuments for *in situ* replacement of their foundations. The necessity of cutting and lifting the monument foundation within limited space introduces significant construction complexity. Hence, the installation of protective platform facilities inevitably imposes forces and dynamic stimuli on the monument, introducing a certain level of safety risk during construction activities. Furthermore, insufficient stiffness of the steel beams may lead to uneven settlement of the monuments, leading to the safety risk of localized damage and overturning during construction activities.

Additionally, the inherent fragility of the monuments, coupled with the aged structures of their foundations and the complexity of subsurface conditions, introduces many unpredictable variables. Lastly, the extraordinary value of the monuments requires minimizing risks associated with construction.

Designing a structural health monitoring system and a monitoring plan, focusing on the overall structure and key areas, becomes an effective means of risk control [16–21]. The relocation project at the Mahavira Hall of Jade Buddha Temple in Shanghai faced challenges such as difficulty in relocation, poor overall structural integrity, and the potential for postural changes and risk in the Buddha statues as cultural artifacts. To ensure the safety of the main structure during the relocation process, an automated, real-time, networked, and integrated monitoring system was designed, providing reliable assurance for the overall translation of the main structure [22]. Therefore, implementing health monitoring throughout the entire process of restoring ancient buildings and cultural relics is imperative [23–25].

Monitoring data can to some extent reflect the posture of the monument, and anomalies in the monument's posture are likely to be manifested in the monitoring data. Therefore, the processing and analysis of monitoring data are paramount. Upon data acquisition, the initial step involves enhancing data quality through tasks such as filling in missing data and identifying anomalies [26]. Subsequently, a comprehensive analysis of the dataset is conducted, including stability and reliability assessments [27]. Finally, information mining and assessment of structural health status are conducted.

In particular, throughout the project implementation, we noted a robust positive correlation between construction activities and monument posture. Subsequently, we endeavored to identify the construction activities from an extensive dataset using data mining techniques. Given the advancements in machine learning, employing sophisticated algorithms for information extraction from this data has become a focal point of research [28–34]. Monitoring data can be effectively mined using various methods, including statistical features [35], modal parameters [36], multi-scale analysis [37], and deep learning [38]. This study has enhanced traditional statistical feature-based methods and, considering the specific nature of the target monitoring project, incorporated unsupervised machine learning to classify the construction activities.

This paper presents a comprehensive overview of the structural health monitoring (SHM) system implemented in the project, with three primary objectives: to acquire the most reliable monitoring data, issue early warnings for potential structural risks, and analyze the structural response based on the collected data. Leveraging the unique characteristics of this project, which involved a substantial volume of multi-source data, the authors developed an innovative unsupervised processing approach based on data fusion, building upon prior research [39].

This study makes significant contributions to bridging the gap between cultural heritage conservation and modern engineering techniques. Moreover, it advances the integration of monitoring data processing with machine learning methodologies. The findings and methodologies introduced in this work offer valuable insights for guiding future monitoring initiatives in translocation projects and enhancing the protective measures for key cultural relics.

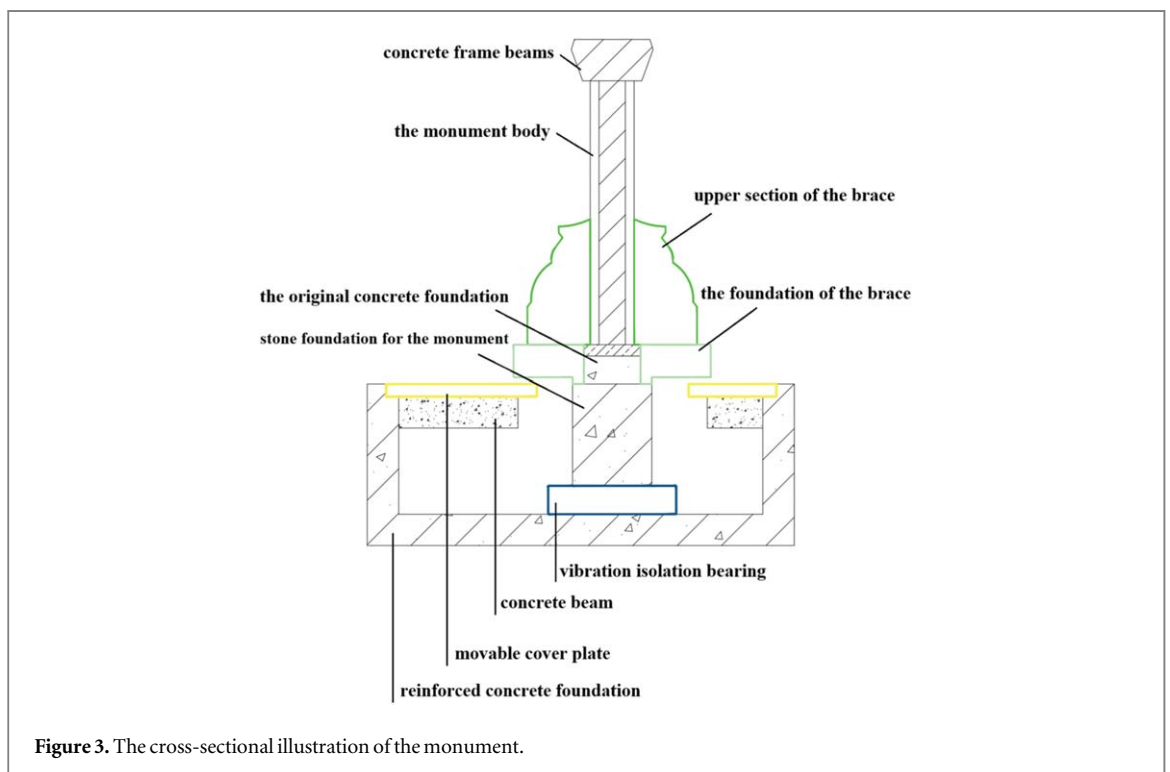
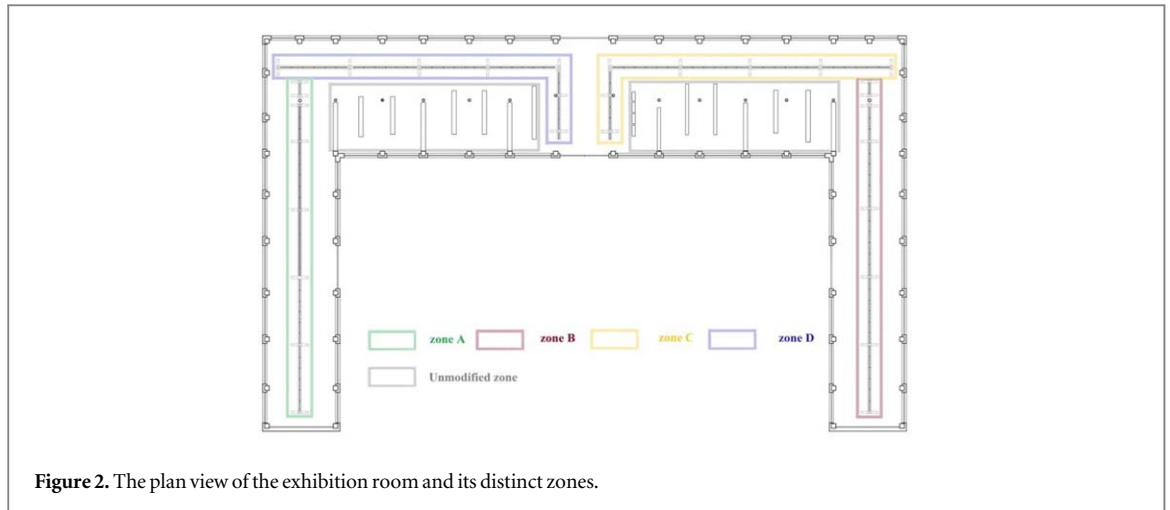
Implementation of isolation replacement

The exhibition room, which has undergone seismic functional upgrading, is shaped like the letter 'n' and has been artificially divided into four zones: Zone A, Zone B, Zone C, and Zone D, as shown in figure 2. Specifically, Zones C and D each feature a set of L-shaped interlocking stone monuments, while Zones A and B comprise a set of north-south-oriented interlocking stone monuments along with a short stone monument.

Each group of monuments comprises the original monument, flanked by two braces, and the upcoming installation of the new vibration isolation foundation section. Specifically, the monument encompasses the monument body, concrete frame beams, stone foundation for the monument, and the original concrete foundation. The brace primarily consists of the upper section of the brace and its foundation. The new vibration isolation foundation mainly comprises two reinforced concrete foundations, the vibration isolation bearing situated between them, and the concrete beam with a movable cover plate. Due to confidentiality concerns regarding the actual structures, this paper focuses on the monitoring techniques and methodologies. Therefore, only schematic diagrams are provided to illustrate the key concepts, rather than detailed depictions of the actual structures, as shown in figure 3.

The primary objective of the seismic performance enhancement construction is to replace the original foundation with a new vibration-isolating foundation while ensuring complete protection of the main section of the monument. Specific monitoring and construction activities were executed successively in four zones. The specific key processes and construction timeline are shown in figure 4 and table 1.

Prior to the seismic performance enhancement, construction simulation underwent testing using a scale model. The crucial monitoring parameters for the construction process were ultimately defined across three



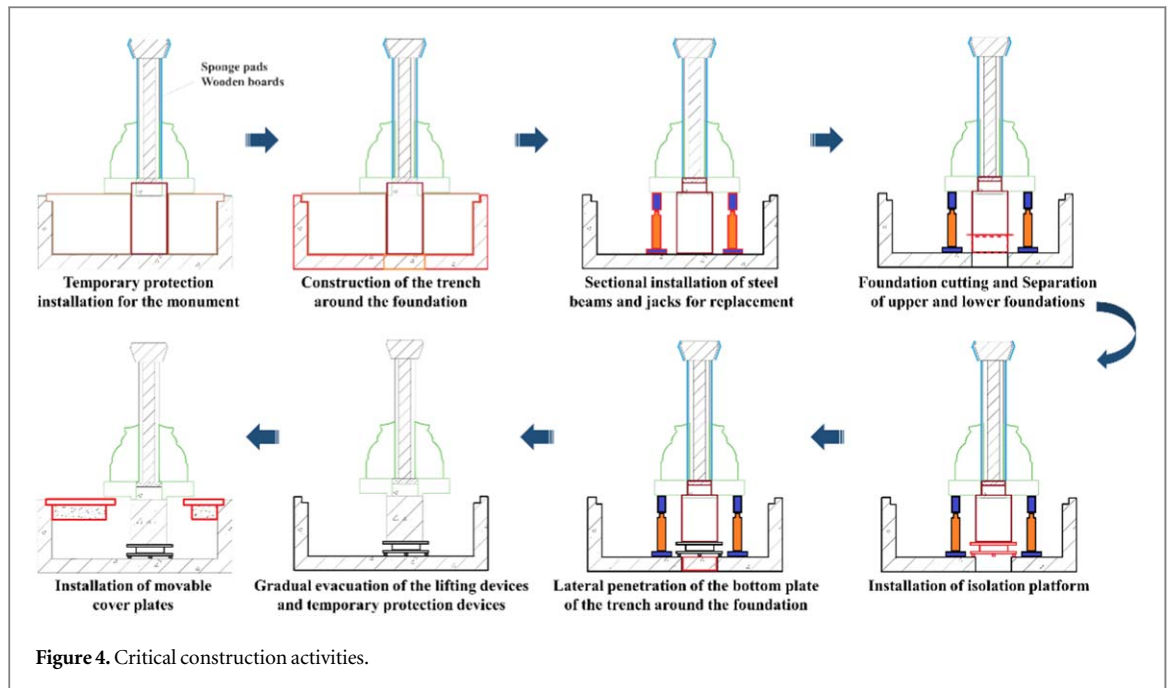
aspects: the overall posture, local deformation, and uneven settlement of the monument, along with the overall tilt of the monument at all stages of construction; the detection of local cracks or deformation in key nodes within the monument's sensitive areas; and the dynamic response of the monument during construction operations, encompassing velocity and acceleration measurements.

Design and deployment of monitoring system

Monitoring system

We have organized the monitoring system into five modules: displacement monitoring, inclination monitoring, acceleration monitoring, crack monitoring, and data acquisition & cloud platform [40, 41], as shown in figure 5. Some monitoring equipment used in the process are shown in figure 6, and the monitoring images are presented in figure 7.

In the displacement monitoring module, following the actual measurement (two laser rangefinders were initially installed in the first construction zone D, but construction dust significantly interfered with instrument measurements, resulting in substantial system errors. Consequently, laser rangefinder data was not chosen for



use), the decision was made to employ level instruments for measurement. Calibration was then supplemented with data obtained from the total station meter.

It is essential to recognize that a level can only measure relative displacement using the formula $S = (S_t - S_0) - (\bar{S}_t - \bar{S}_0)$. Where, S represents the cumulative settlement; S_t represents the current time measurement value of the measurement point; S_0 represents the initial time measurement value of the measurement point; \bar{S}_t represents the current time measurement value of the datum. \bar{S}_0 represents the initial time measurement value of the reference point. We also performed additional calibration and calculated the absolute displacement of the measured points by means of the total station. Detailed information on the level instrument and wireless inclinometer can be found in table 2.

In the inclination monitoring module, we opted for a wireless, low-power, high-precision inclinometer due to its flexible arrangement. Additionally, a more stable wired inclinometer was selected as a supplement for some of the points. The meaning of each angle is shown in figure 8.

The definition of positive and negative is illustrated in the figure: the x -axis is negative if above the horizontal plane and positive if below the horizontal plane; the y -axis is negative if above the horizontal plane and positive if below the horizontal plane; the z -axis exhibits a positive angle above the horizontal plane and a negative angle below the horizontal plane.

Acceleration is monitored using magnetic-electric velocity (acceleration) sensors and a centralized low-speed online monitoring system following on-site measurements for stone monument crack monitoring (real-time monitoring by cameras does not fulfill on-site stone monument protection requirements), the digital camera photography method has been ultimately chosen for recording. Subsequently, a crack identification algorithm is employed to identify and monitor the expansion of cracks. Detailed information on the acceleration monitoring module and digital camera can be found in tables 3 and 4.

The data acquisition and cloud platform module primarily involve consolidating data from the field level instruments and inclinometers through the intelligent acquisition base station. Ultimately, all data is uploaded to the cloud platform, as shown in figure 9. Detailed information on the intelligent acquisition base station can be found in table 5.

Layout of sensors

As previously mentioned, the entire construction area under monitoring is subdivided into four zones: A, B, C, and D. Different types of sensors are strategically placed in each zone and are named in the format 'Sensor type' - 'Layout zone' - 'Number'. Here, 'SZ' represents a level instrument, 'QX' represents an inclinometer, and 'LF' designates the monitoring position for cracks on the monument surface. For example, 'SZ-D-02' signifies the second level instrument positioned in zone D.

Displacement is primarily gauged using level instruments, supported by the total station for supplementary monitoring. Inclination is mainly assessed through a wireless, low-power, high-precision inclinometer, with additional wired inclinometers ensuring data integrity at specific points. The distribution across zones is as

Table 1. Construction and monitoring of key processes and moments.

	Zone D	Zone C	Zone B	Zone A
Temporary protection installation for the monument	Completed by February			
Installation of structural health monitoring system	Feb. 28th ~ Mar. 1st	Feb. 28th ~ Mar. 2nd	Apr. 1st ~ Apr. 2nd	Apr. 1st ~ Apr. 2nd
Jacks Installation	Feb. 26th	Feb. 27th	Apr. 23 rd	Apr. 26th
Cutting of the original foundation	Mar. 2nd ~ Mar. 4th	Mar. 5th ~ Mar. 9th	Apr. 23 rd ~ Apr. 25th	Apr. 27th ~ Apr. 29th
Removal of concrete foundations	Mar. 3 rd ~ Mar. 5th	Mar. 11th ~ Mar. 17th	Apr. 25 rd ~ Apr. 27th	Apr. 30th ~ Mar. 2nd
Excavation to the bottom of the bedding	Completed by Mar. 6th	Completed by Mar. 19th	Completed by Apr. 30th	Completed by May. 3 rd
Chiseling of foundations	Completed by Mar. 7th	Completed by Mar. 19th	Completed by Apr. 28th	Completed by Apr. 30th
Rebar tying and concrete pouring	Completed by Mar. 15th	Completed by Mar. 22nd	Completed by May. 6th	Completed by May. 4th
Installation of seismic isolation bearings	Mar. 19th	Mar. 26th	May. 6th	May. 8th
Remove the jacks	Mar. 24th	Mar. 29th	May. 9th	May. 12th
Sensor removal		Mar. 26th		May. 25th

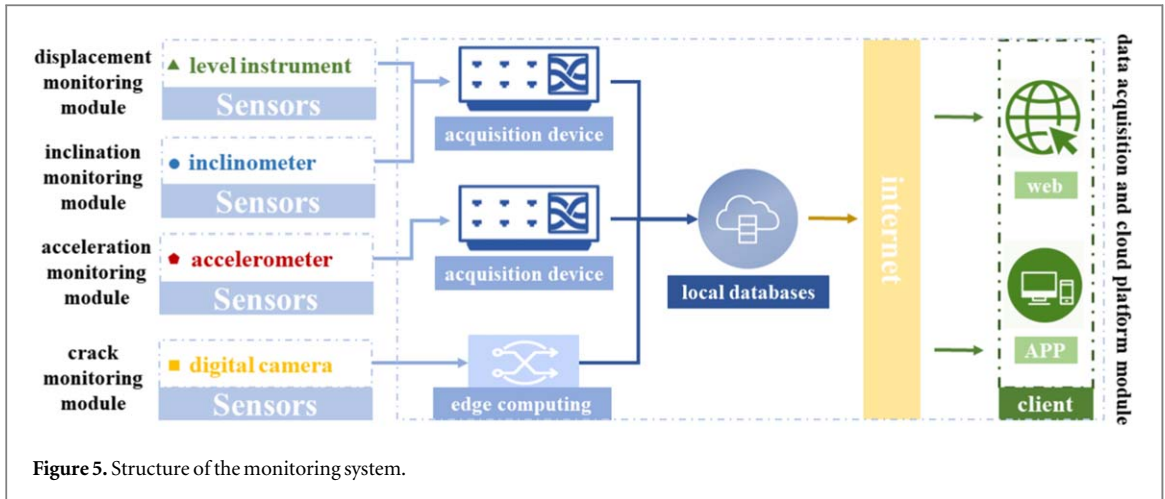


Figure 5. Structure of the monitoring system.

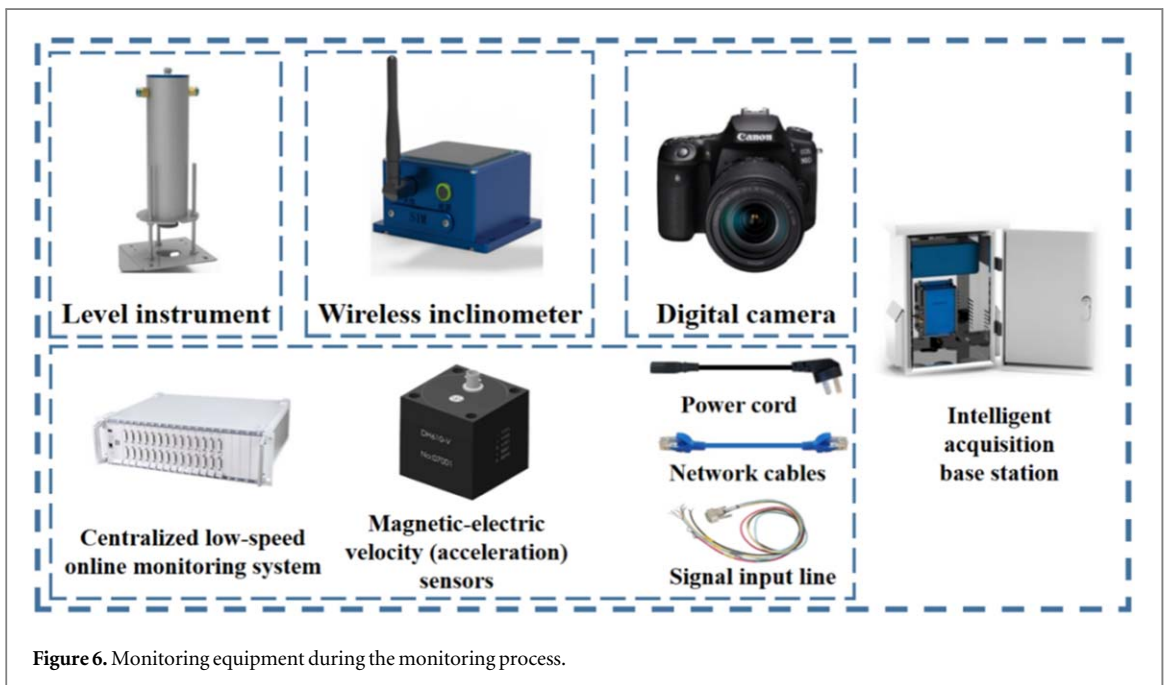


Figure 6. Monitoring equipment during the monitoring process.

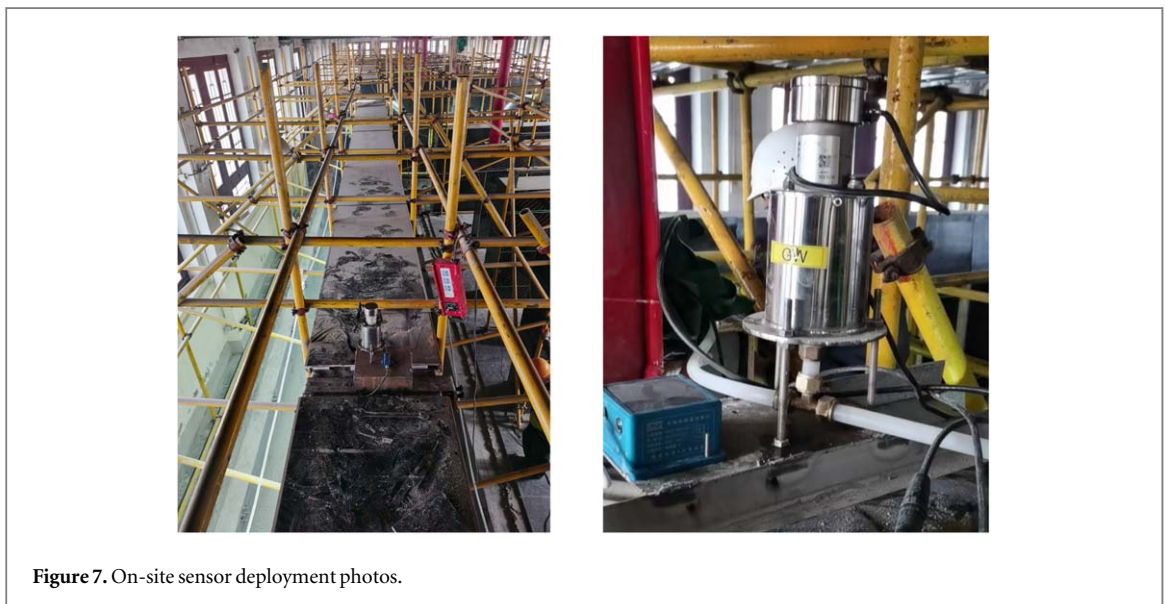


Figure 7. On-site sensor deployment photos.

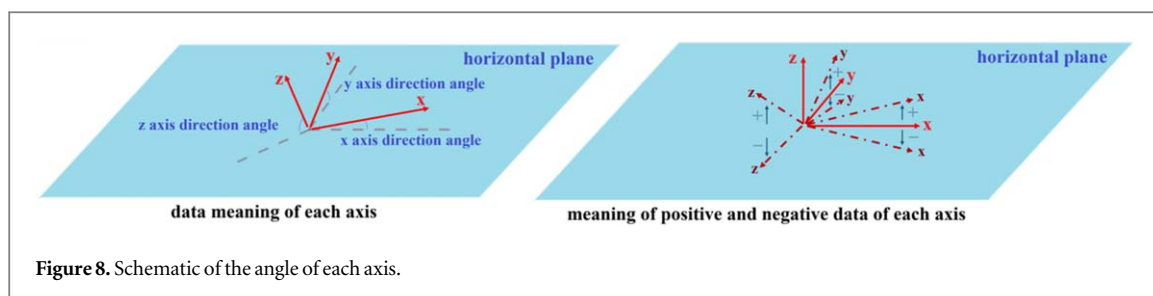


Figure 8. Schematic of the angle of each axis.

Table 2. Parameters of the level instrument and wireless inclinometer.

	Precision	Sensitivity	Voltage	Power dissipation	Protection class
Level instrument	0.1 mm	0.01 mm	DC 5 ~ 30 V	<0.05 W	>IP67
Wireless inclinometer	$\pm 0.005^\circ$	<0.001 $^\circ$	DC 5 V (Type-C)	<0.2 W	>IP67

Table 3. Parameters of the acceleration monitoring module.

Centralized low-speed online monitoring system					
Highest continuous sampling rate	Frequency response range		Operating temperature		Protection class
200Hz	DC ~ 30 Hz		-10 ~ 50 $^\circ\text{C}$		IP50
Magnetic-electric velocity (acceleration) sensors					
Switch of gear	Sensitivity	Range	Frequency response		Operating temperature
0	$0.3\text{V m} - \text{s}^{-2}$	20ms^{-2}	$\pm 10\%$ 0.5 ~ 50 Hz	-3 ~ +1 dB 0.25 ~ 100 Hz	-10 $^\circ\text{C}$ ~ + 60 $^\circ\text{C}$
1	$20\text{V}/\text{ms}^{-1}$	0.125ms^{-1}	4 ~ 80 Hz	1 ~ 100 Hz	
2	$5\text{V}/\text{m}\cdot\text{ss}^{-1}$	0.3m s^{-1}	1 ~ 80 Hz	0.5 ~ 100 Hz	
3	$0.3\text{V}/\text{ms}^{-1}$	0.6m s^{-1}	0.5 ~ 80 Hz	0.17 ~ 80 Hz	

Table 4. Parameters of the digital camera.

Digital camera				
Effective pixels	Image processor	Maximum resolution	Range of focus	Aperture range
32500000	DIGIC 8	6960×4640	18-135 mm	F3.5-F5.6

follows: Zone A has 7 level instruments and 7 inclinometers from north to south, Zone B has 6 of each arranged likewise, Zone C features 7 level instruments and 4 inclinometers from east to west, and Zone D includes 7 level instruments and 3 inclinometers from west to east. The arrangement of the level instruments and inclinometers is shown in figures 10 and 11.

Acceleration (speed) measurements were not monitored in real time but through flexible monitoring with real-time changes in monitoring positions during key construction processes.

For image monitoring (crack monitoring), the selected points are shown in figure 12.

It is crucial to underscore that monitoring data should be preserved in their raw and unprocessed state. Before analysis, the monitoring data should undergo checks, evaluations, and necessary processing, including the elimination of abnormal data, repair of missing data, trend removal, digital filtering, and noise reduction.

By monitoring the static response and dynamic response of the structure during the displacement process under various working conditions, displacement phases, and environmental excitation, it becomes possible to comprehensively monitor and provide warnings for the entire process of structure displacement. Monitoring stresses in key parts and components of the structure during the displacement stage, along with observing the overall attitude and local uneven settlement, enables a multi-level alarm system for critical monitoring data.

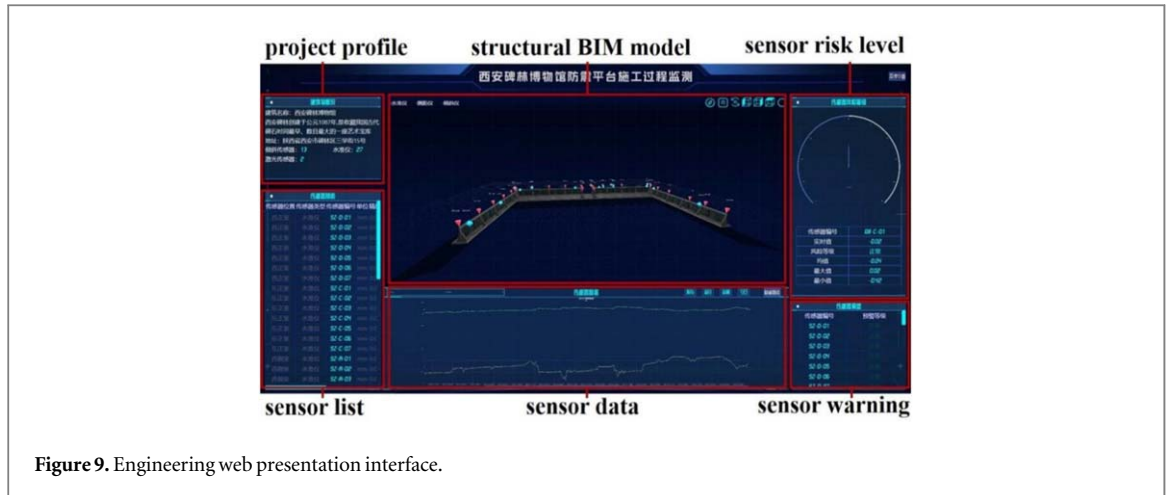


Figure 9. Engineering web presentation interface.

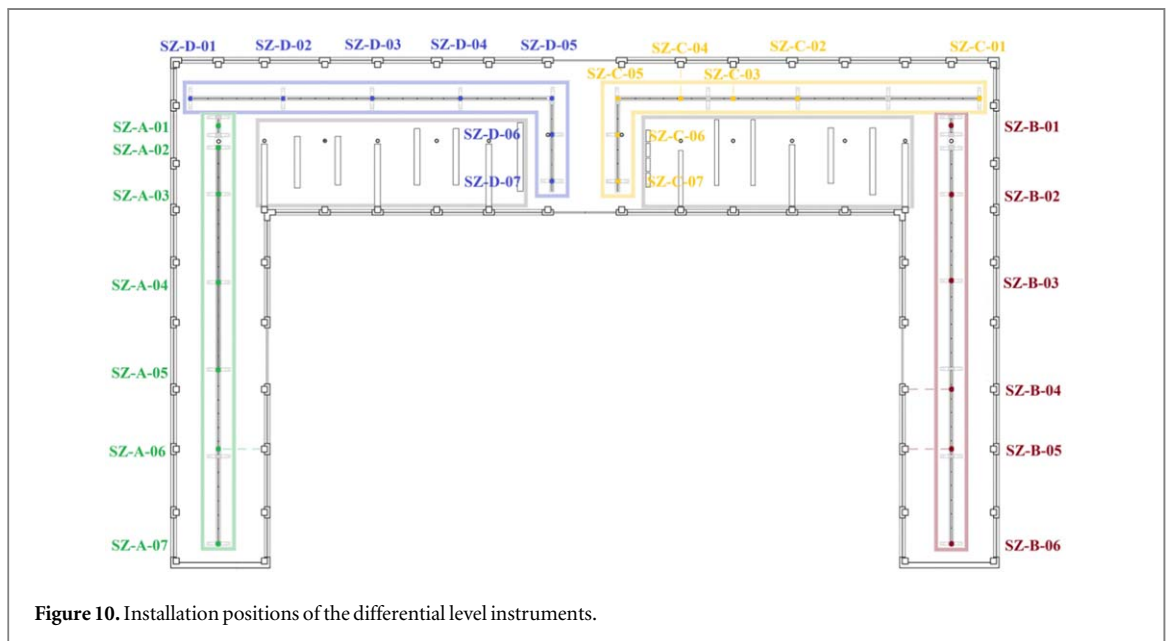


Figure 10. Installation positions of the differential level instruments.

Table 5. Parameters of the intelligent acquisition base station.

Intelligent acquisition base station			
Voltage	Output voltage and power	Specification	Protection class
DC 12 ~ 30 v	DC 12/24V– 20 W	160*120*65 (mm)	>IP66

The overall attitude, local settlement, and deformation data of the structure should be designated as observation time points, with the initial monitoring values serving as benchmark data. Correlations should be established with relevant data from structural safety inspections conducted prior to the shift, and attention should be directed toward the incremental change of monitoring data relative to the initial observation values during the monitoring phase.

At key time points corresponding to structural system transformations during the shifting process, several reference time points should be set. Reference benchmark values for the observation data of the corresponding states should be established, and incremental changes relative to different reference time points should be

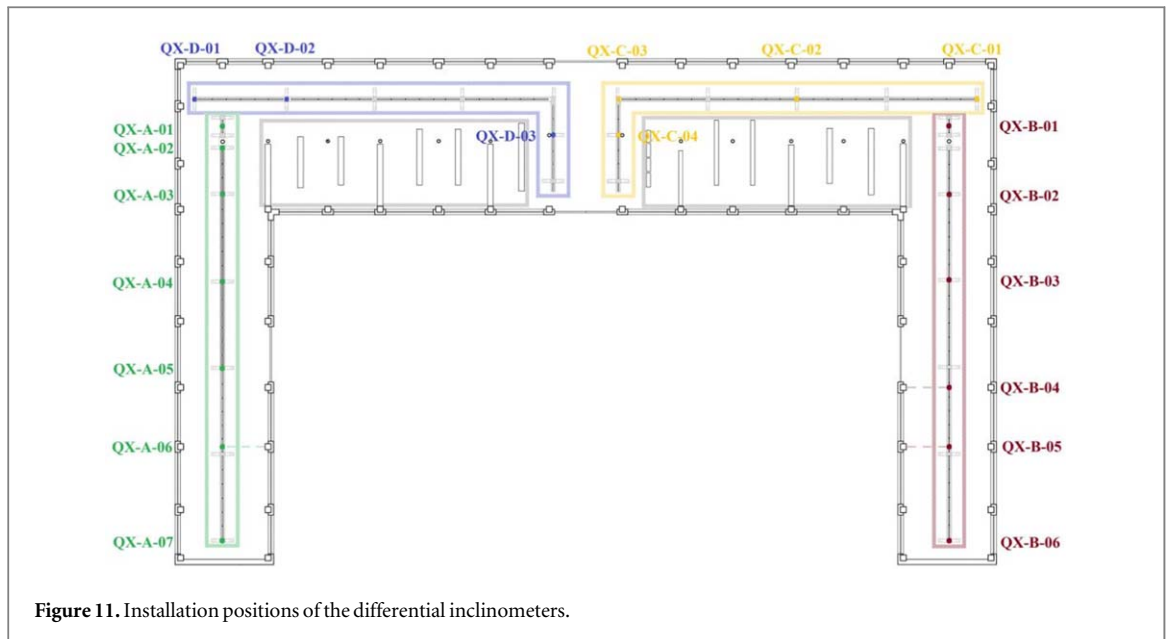


Figure 11. Installation positions of the differential inclinometers.

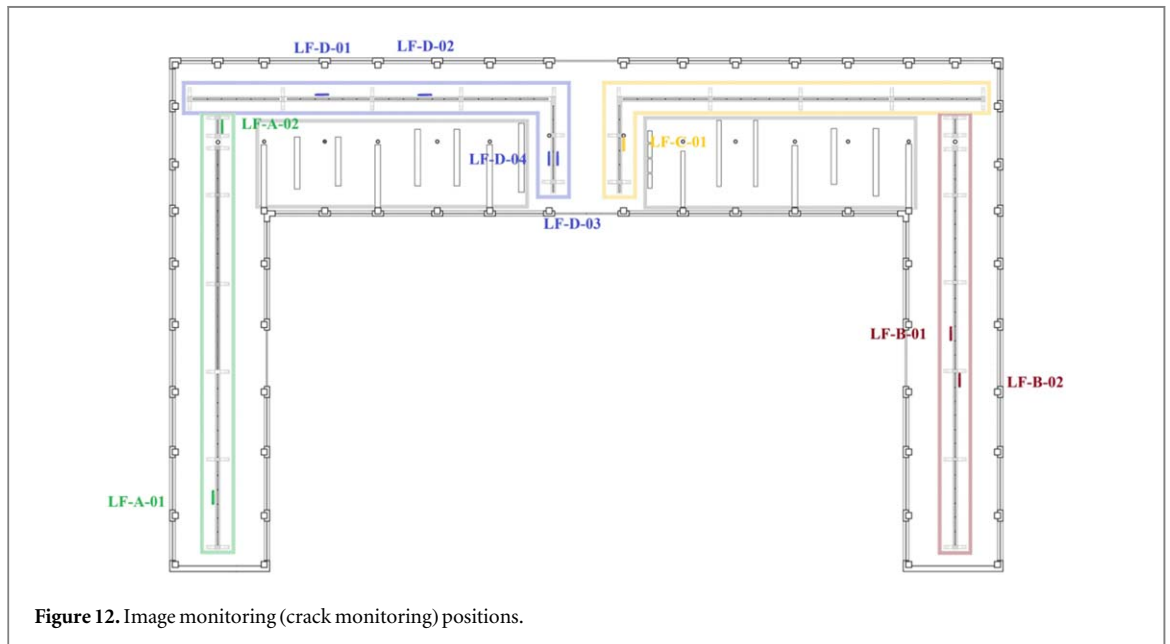


Figure 12. Image monitoring (crack monitoring) positions.

analyzed in subsequent stages. Consequently, daily, weekly, and monthly reports are generated to meet the varying needs of displacement monitoring at different stages.

Installation of sensors

During the installation process, it is imperative to secure the artifacts as securely as possible, ensuring no damage to them, to obtain more accurate data. Specifically, level instruments and inclinometers are affixed to the top of the monument using a hoop, with felt padding between the hoop and the monument. Accelerometers are fixed in the measured area using cleanable rubber cement when testing is required. For points requiring crack monitoring, a window is opened, and a foam protective layer is set up. All sensor installation methods are compiled into a comprehensive program, submitted to the relevant management department for approval and adoption.

Additionally, attention is given to photographic records of each point, recognizing that the installation direction of inclinometers significantly impacts the data's interpretation.

Setting warning and alarm values

Based on consultations with experts, relevant departments, and management units, the warning and alarm values are detailed in table 6.

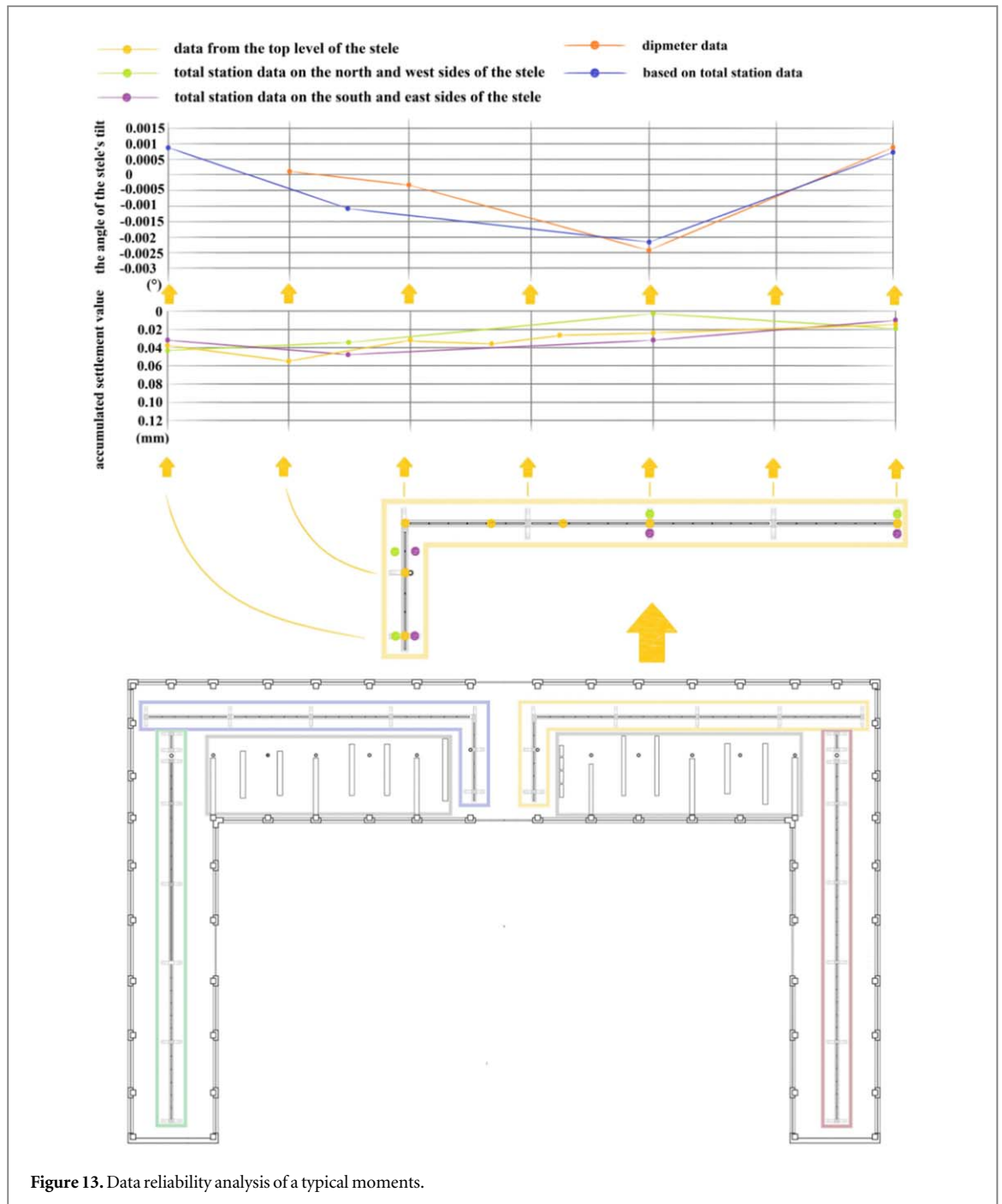


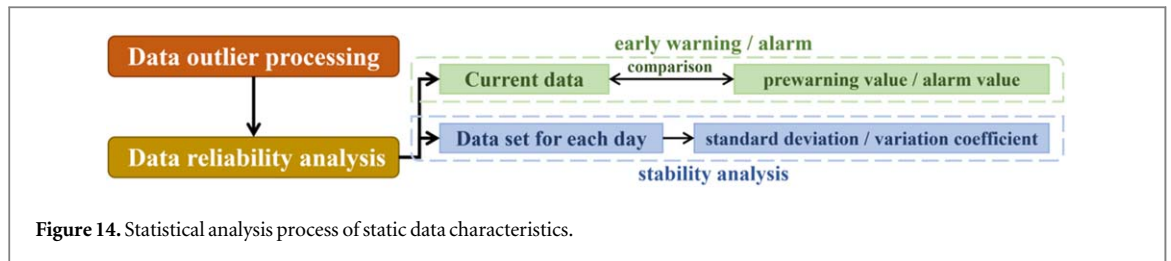
Figure 13. Data reliability analysis of a typical moments.

Unsupervised classification of construction state

Data validation

Given the presence of multiple total station measurement points situated on both sides of the monument, data from the level instrument, inclinometer, and total station measurements during typical time periods are regularly selected for comparison and analysis throughout the monitoring process. This is undertaken to verify the accuracy of the data. As an illustration, consider the data from March 18, between 8:30 and 11:30 a.m. in Zone D, as shown in Figure 13.

It is evident that the inclination values derived from the total station data on both sides of the monument align closely with the data measured by the inclinometer on the top of the monument. Similarly, the settlement values deduced from the total station data on both sides of the monument are in good agreement with the data measured by the level meter on the top of the monument. The mutual confirmation between the level instrument, inclinometer, and total station establishes the reliability of the data.

**Table 6.** Warning and alarming values in monitoring process.

Data type	Warning value	Alarming value	Remarks
inclination	0.02°	0.05°	Based on expert consultation and project guidelines
settling	0.1mm/d	0.2mm/d	Daily difference, defined by management unit
differential settlement	0.2mm	0.4mm	Based on adjacent station comparison, expert input
crack length (increment)	0.2mm	0.5mm	Selected typical location, derived from initial measurements
acceleration	0.02g	0.05g	Based on top of stone monuments, established criteria

Table 7. Data anomalies and handling methods.

Type of data anomalies	Data characteristic	Treatment
Abnormal datum instrument readings	All data points produce the same change of greater magnitude	Filtering with filtering algorithms
Changes in the instrument due to changes in the external environment	All data points produce a small change, which soon recovers	Analyze the amount of environmental impact and subtract the abnormal
Instrumental system errors (e.g., air bubbles in water lines)	A change at one point is followed shortly by a change at all other points.	Analyze the amount of systematic error effects, subtracting the anomalies
construction disruption	A large change in a point location, but no change in total station detection	Calibration of the value against total station data

Exception judgment and outlier handling

In the analysis process, the initial step involves excluding outliers and retaining data that best represents the monument's changes. To achieve this, we have categorized various anomalies based on actual observations and proposed corresponding processing methods for different anomalies, as shown in table 7.

Statistical analysis of static data characteristics

As it is necessary to assess the condition of the monument on a daily basis and generate reports for submission to the relevant departments, the following flow-based static data analysis process (shown in figure 14) has been formulated. Real-time anomalies are identified and rejected from the data after obtaining it. The reliability of the data is then analyzed by selecting a typical period each week, as described in the first part of this section. For the real-time data changes, a comparison with the warning and alarm values is conducted to achieve real-time monitoring. For the entire day's monitoring data set, statistical indicators such as standard deviation, coefficient of variation, and others are calculated to analyze the stability of its data within the day.

Unsupervised classification of working state

With the development of intelligent algorithms, in addition to simple limit-based judgments and some traditional statistical algorithms, we use intelligent algorithms to analyze and evaluate the data obtained from structural health monitoring. Common methods in existing research include prediction and warning of future data based on RNN (or improved networks like GRU) and historical data [42], structural damage identification based on CNN and images [43, 44], and structural comfort and safety assessment based on Bayesian networks [45, 46]. However, most commonly used methods are supervised machine learning algorithms, which face challenges in being overly reliant on manual labeling to construct complete data sets. Therefore, we have opted for unsupervised algorithms to address subsequent structural health assessment problems, as shown in figure 15.

According to the actual project, the data obtained from the zone C was the most complete in all channels and all times. Therefore, the data from zone C was chosen as an example to be processed to examine the validity of the method. Figure 16 is a flow chart of the experiment using actual data.

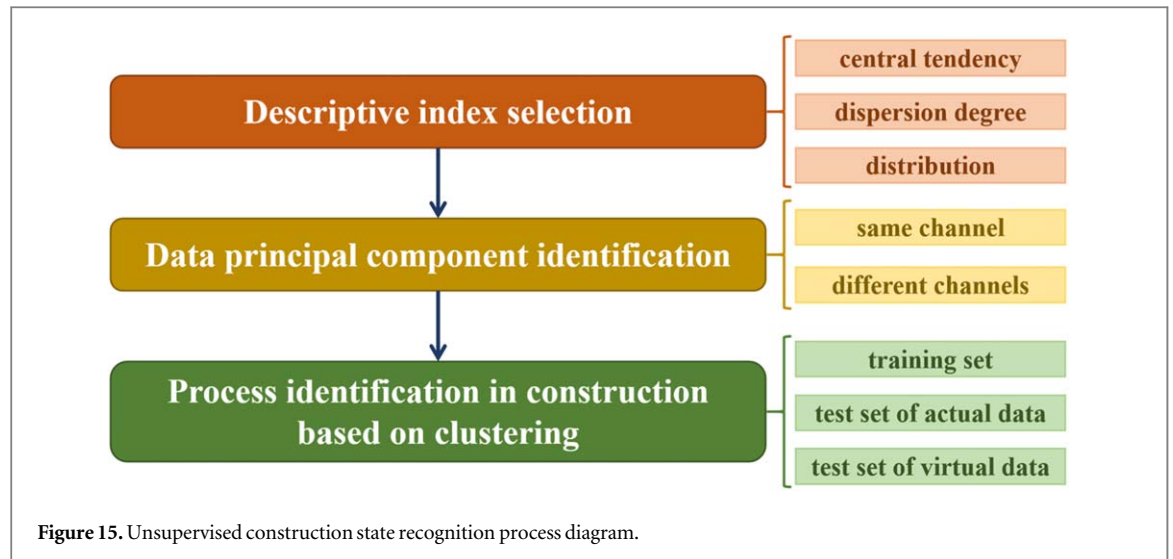


Table 8. Correspondence between clustering results and construction status.

	Number	Temporal characteristics	Data characteristics
class 1	160	Cutting the whole foundation or chiseling and removing the concrete, which does not act directly on the monument.	The north and south ends of the monuments have obvious variations, with the extreme difference ranging from 0.05 mm to 0.4 mm, and the central part has more obvious variations with the extreme difference ranging from 0.05 mm to 0.2 mm.
class 2	26	Perform foundation drilling or monument foundation removal for a specific point of the monument.	The north and south ends of the monuments have more obvious variations with extreme differences of 0.1 mm ~ 0.2 mm, and the center has obvious variations with extreme differences of 0.15 mm ~ 0.35 mm.
class 3	63	No construction in the vicinity of the object monument that has a significant impact on the monument throughout the day (day and night)	All monitoring locations are within 0.1 mm of the range of change.
class 4	3	Construction is concentrated in the central area, where significant changes are observed.	Localized extremes of 0.5 mm or more
class 5	2	Construction is concentrated in the north side, where significant changes are observed.	Localized extremes of 0.5 mm or more
class 6	1	Construction is concentrated in the south side, where significant changes are observed.	Localized extremes of 0.5 mm or more

The level instrument datasets from 2023.4.12.0:00 to 2023.4.29.24:00 in zone C serve as the training set. Initially, all data in the training set undergo calibration with the inclinometer and total station to acquire corrected data. The time dimension is segmented into hourly intervals, and the relative elevation change data between two adjacent level positions constitute different channels in the spatial dimension. For instance, the dataset ‘2023.4.12 00:00 → 2023.4.12 01:00’ for the channel ‘SZ-A-02-SZ-A-01’ illustrates the variations in elevation difference between point 2 and point 1 in Zone C from 0:00 to 1:00 on April 12, 2023 (given that actual level readings are taken every five minutes, resulting in 11 data points per set). Three steps are executed on the training set obtained from this collation.

The initial step involves the selection of descriptive indices. Data description statistics primarily encompass three facets: trend concentration (plurality, mean, median), dispersion degree (maximum, minimum, extreme deviation, variance, standard deviation, coefficient of variation), and distribution (kurtosis and skewness). Given the nature of the data, the mean is chosen as a representative value for the data set trend. Through the analysis of the inherent meaning and correlation among these representative values, a more pronounced correlation is observed among the maximum value, minimum value, and extreme deviation, while the variance, standard deviation, and coefficient of variation exhibit a stronger correlation. Consequently, extreme deviation and standard deviation are chosen as the characterizing values for dispersion degree. Considering the limited data in each data set, the data distribution is not taken into account. In summary, mean, extreme deviation, and standard deviation are selected as the representative values for each data set. Practically, the mean reflects the

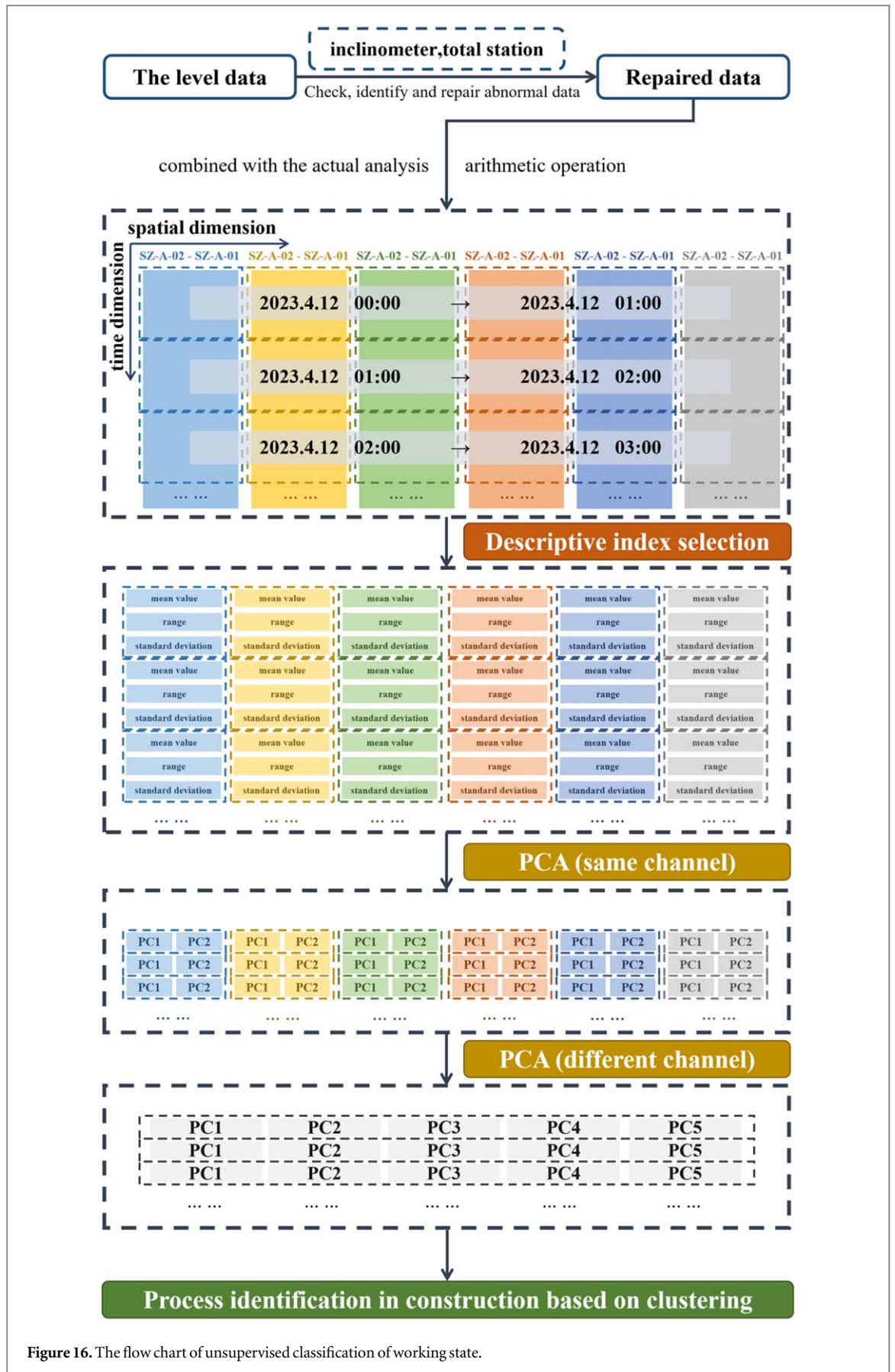
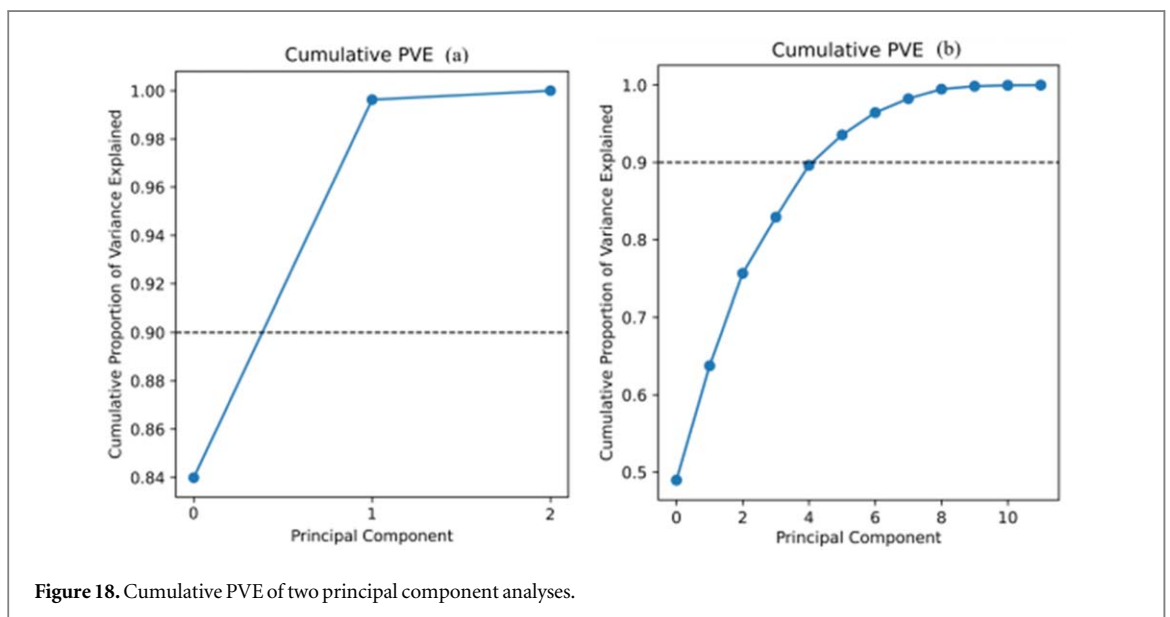
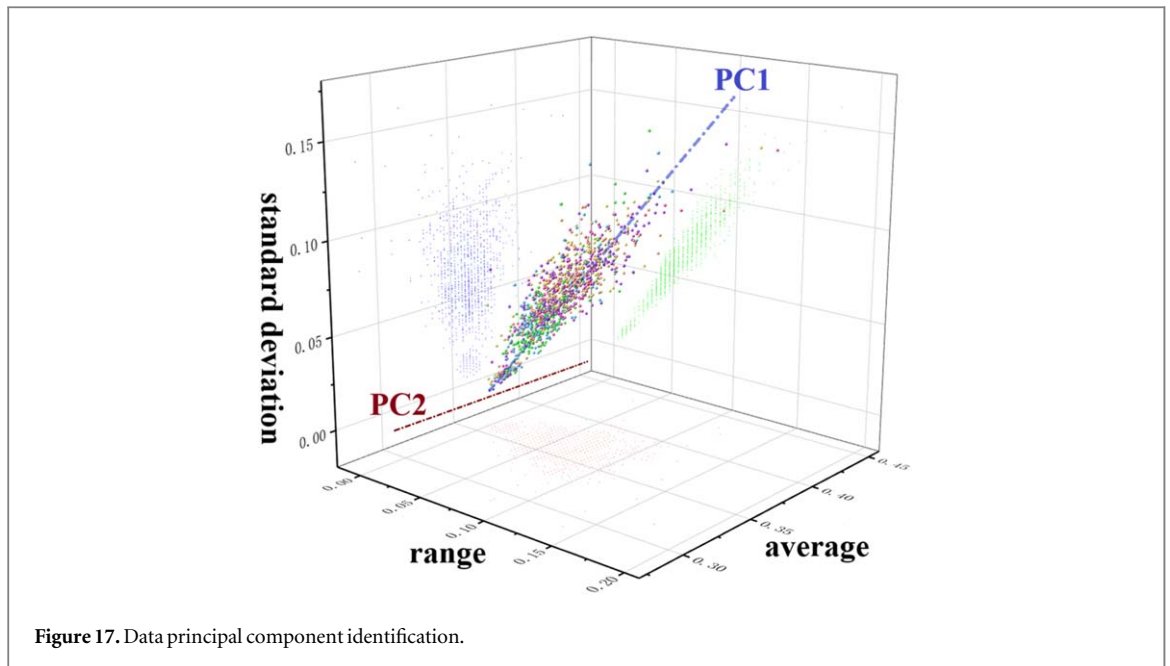


Figure 16. The flow chart of unsupervised classification of working state.



magnitude of change in the data over time, positively correlated with the cumulative change over that period. The extreme deviation mirrors the maximum range of change within the time frame, and the standard deviation indicates the degree of dispersion of the change over the temporal range. These three values capture the indicators of interest. Following descriptive metrics statistics, each dataset is replaced with these three statistics, providing a more explicit representation of the relationship indicators while significantly reducing the data volume.

The second step involves the identification of data principal components (PCA). The PCA method systematically identifies the primary directions of variation within the dataset and projects them onto a new coordinate system. The first principal component captures the maximum variance present in the data, followed by the second principal component, which captures the second-highest variance orthogonal to the first. This process continues iteratively, unfolding subsequent principal components. Upon actual calculation, a robust correlation persists among the mean, extreme deviation, and standard deviation, especially evident in datasets with a limited sample size, where extreme deviation and standard deviation exhibit a pronounced linear relationship, as shown in Figure 17. To address this, the three statistically descriptive values are initially represented by their first two principal components within each set of clusters, achieving an explanatory rate exceeding 99%, as shown in figure 18 (Cumulative PAE(a)). This process results in six channels for each unit time band, each comprising two data points. Subsequently, a principal component analysis is applied to these 12 data

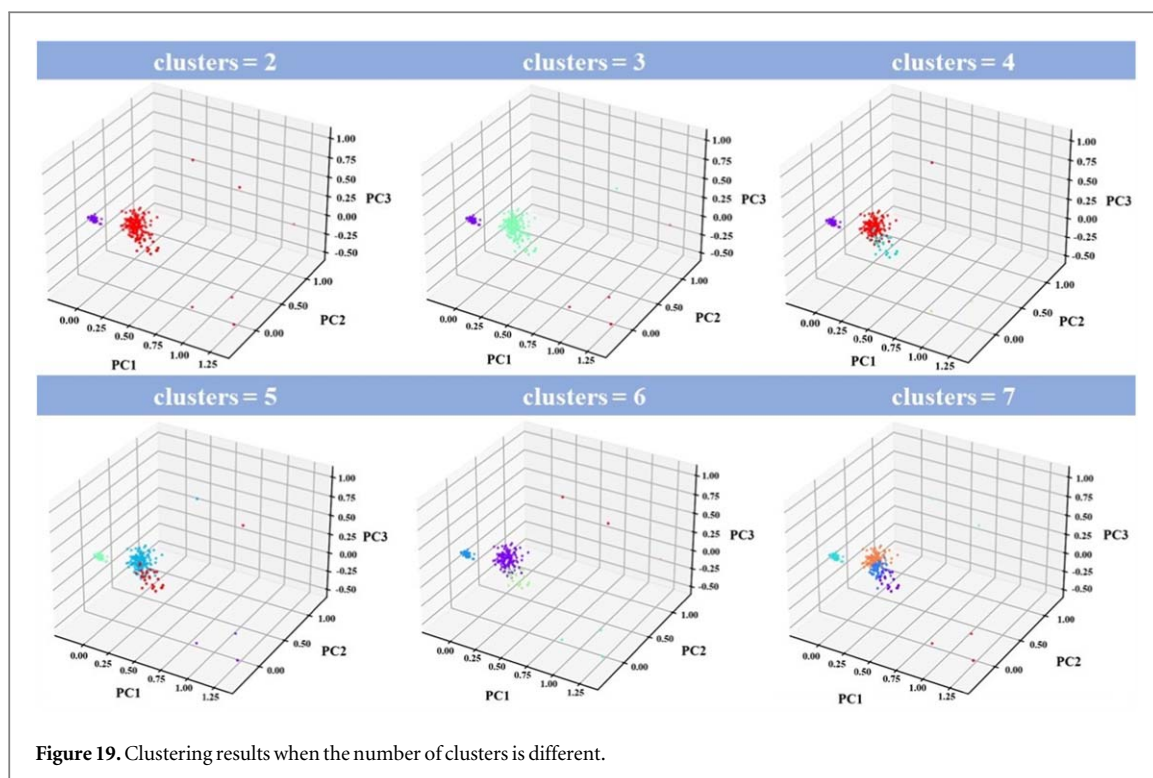


Figure 19. Clustering results when the number of clusters is different.

points, revealing that the first five principal components can adequately explain approximately 90% of the variance, as shown in figure 18(Cumulative PAE(b)). In practical terms, the mean indicates whether these displacement differences tend to shift in a particular direction or remain generally stable, while the variance reflects the consistency or dispersion of these differences, revealing whether there are significant fluctuations in displacement between points. Consequently, the first five principal components are selected to characterize the state of the monuments in the western chamber during that specific time period.

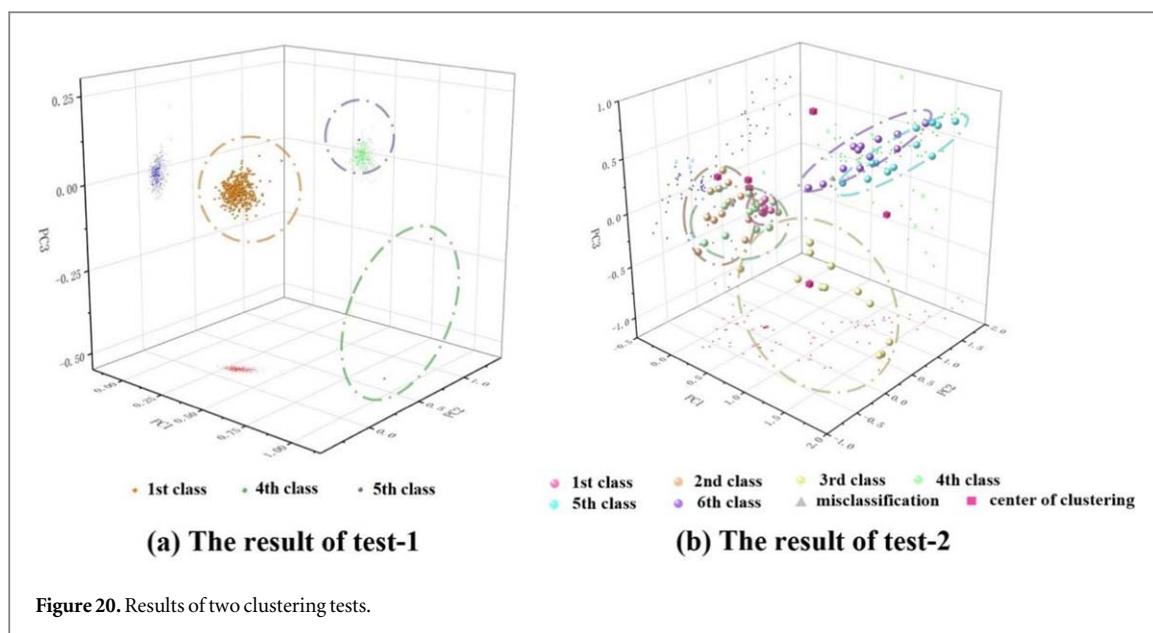
The third step involves clustering from construction process recognition. Initially, clustering is executed based on the data set generated in the previous step, utilizing 2, 3, 4, 5, 6, and 7 clusters, respectively, as shown in figure 19. Upon comparison with the actual data and corresponding construction scenarios, it is observed that classification is insufficient when divided into 2, 3, 4, and 5 classes. Simultaneously, there is redundancy when divided into 7 classes. Consequently, the clustering method with a classification of 6 classes is chosen.

Upon comparing the clustering results with the construction conditions documented in the field, it was observed that the construction status of each category aligns more accurately with the observed features, as shown in table 8.

The experimental data for the west side chamber spans from 2023.4.30.0:00 to 2023.5.21.24:00. However, given that most of the foundation construction work in the west side chamber had concluded between 2023.4.12.0:00 and 2023.4.29.24:00, the subsequent time periods exhibited smoother trends without misrecognition. Exceptions were noted during three time intervals in the central and northern areas related to earth excavation before the third day of May, where significant variations occurred but remained below the alarm threshold. To supplement Experiment 1, the algorithm generated datasets corresponding to the six types of engineering conditions, each comprising 12 sets of data. These sets underwent clustering through the machine learning process. Only three points were misidentified during recognition, resulting in a recognition efficiency exceeding 95%. It's noteworthy that the misidentified points were concentrated near the intersection of two classes, suggesting the effectiveness of the earlier training process.

Moreover, both Experiment 1 and Experiment 2 exhibit shortcomings in the data. The data in Experiment 1 is evidently insufficient, yet it aligns more closely with the actual scenario. Conversely, the data generated by the algorithm in Experiment 2 deviates somewhat from the actual data. This discrepancy affects the clustering center, which does not consistently align with the midpoint of each class. However, these two experiments complement each other, compensating for their respective shortcomings and strengthening their overall findings, as shown in figure 20. The combined recognition efficiency exceeds 98%.

In conclusion, the unsupervised machine learning intelligent discrimination method proposed by us can be effectively applied in engineering, complementing real-world scenarios. This approach offers valuable insights for the advancement of intelligent engineering health monitoring.



Vibration characterization and structural dynamic response in construction-focused processes

Characterization of vibration during construction

In light of the meticulous attention required for heritage preservation efforts, the vibration excitation during key processes necessitates thorough testing and analysis before construction commences. Three sets of control experiments were simulated for each construction process (shown in table 9), observing vibrations on the ground, the steel beam at the base of the monument, and the top of the monument. Among all construction processes, the use of an electric breaker during concrete breaking generated the most significant vibration excitation as shown in table 10. Therefore, this section focuses on the data obtained from simulating concrete breaking with an electric breaker as an illustrative example.

The first set of experiments measured acceleration in three directions east-west, north-south, and vertical, on the ground near the crushed concrete block (corresponding to test-1-1, test-1-2, test-1-3). Despite a slight tremor being perceptible on the ground near the concrete block undergoing breaking, the maximum accelerations remained below 0.02 g.

The second set of experiments gauged the dynamic response on a steel beam at the base of the monolith near the crushed concrete block (corresponding to test-2-1, test-2-2, test-2-3). When the electric pick was employed for the concrete breaking work, the vibration acceleration of the steel beam at the bottom of the monument increased significantly compared to other construction processes but remained smaller than the first group of experimental data.

The third set of experiments measured the dynamic response of the top of the monument near the crushed concrete block (corresponding to test-3-1, test-3-2, test-3-3). Due to the lesser restraint at the top of the monument, the acceleration in both horizontal directions exceeded that recorded when the sensor was placed on the steel beam at the bottom of the concrete. However, it still remained below the levels observed in the first set of data and well below the warning value.

Measurement of structural dynamic response

As previously mentioned, the structural dynamic response was not monitored in real time but rather by focusing on key construction nodes. The following details some of the monitoring work carried out in Zone D, which was the initial construction zone. Figure 21 shows the distribution of acceleration monitoring points in zone D.

Arrange two horizontal acceleration sensors, JSD-D-01 and JSD-D-02, along with one vertical acceleration sensor, JSD-D-03, on the tops of the first and second sets of monuments. The horizontal acceleration along the short side of the monument surpasses the vertical and the horizontal acceleration along the long side but essentially remains below $0.03m/s^2$, which is under the preset alarming value of 0.02 g.

Position two horizontal acceleration sensors, JSD-D-04 and JSD-D-05, along with one vertical acceleration sensor, JSD-D-06, at the top of the middle of the first group of monuments. The cutting begins at the intersection of the first and second monuments from west to east until the cutting of the second monument is completed. The maximum values of east-west and vertical acceleration are approximately $0.017m/s^2$, while the

Table 9. Response of broken concrete to different locations.

Serial number	Accelerating curve	Scene picture
test-1-1		
test-1-2		
test-1-3		
test-2-1		
test-2-2		
test-2-3		

Table 9. (Continued.)

Serial number	Accelerating curve	Scene picture
test-3-1		
test-3-2		
test-3-3		

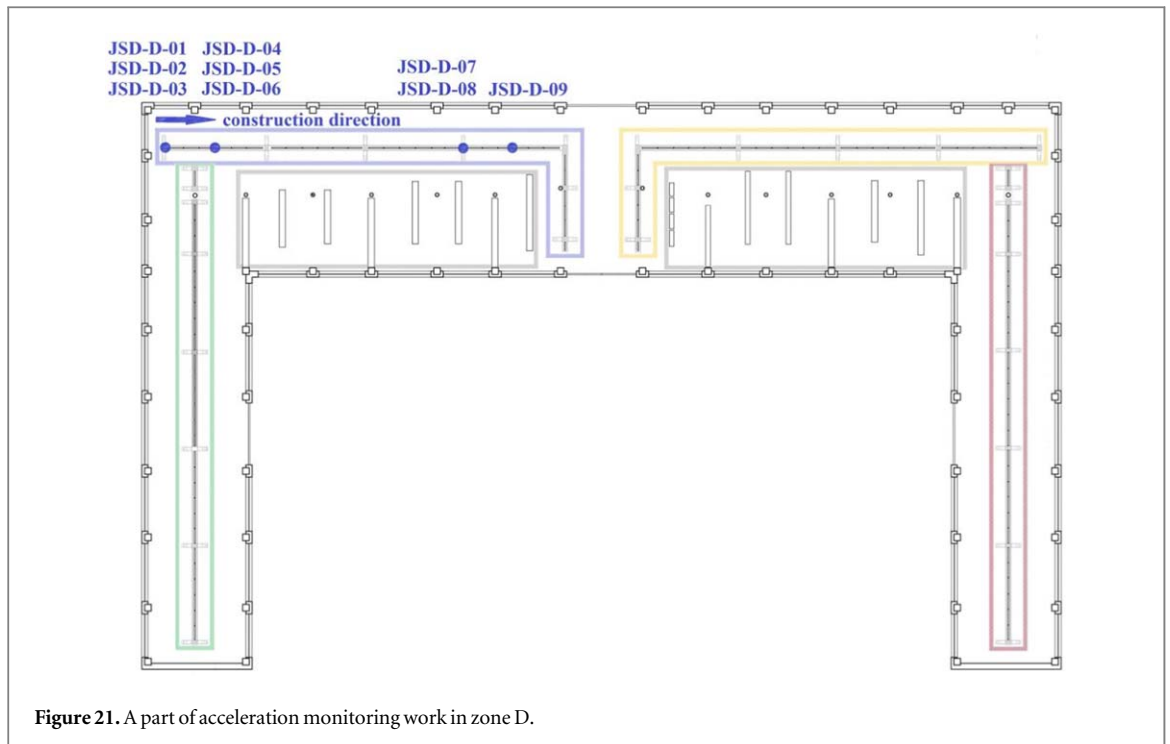


Figure 21. A part of acceleration monitoring work in zone D.

Table 10. Maximum values of acceleration at different positions when breaking concrete.

Measuring direction	Group I	Group II	Group III
horizontal acceleration in the north-south direction	0.047 m/s^2	0.012 m/s^2	0.024 m/s^2
horizontal acceleration in the east-west direction	0.096 m/s^2	0.012 m/s^2	0.037 m/s^2
vertical direction	0.162 m/s^2	0.042 m/s^2	0.045 m/s^2

north-south direction, along the short axis of the monument, being less constrained, results in a larger acceleration with a maximum value of about $0.033m/s^2$. All these values remain below the set warning threshold.

On the east side of Zone D, position a vertical acceleration sensor, JSD-D-07, and a horizontal acceleration sensor, JSD-D-08, in the north-south direction, along with another vertical sensor, JSD-D-09. Between 10:38 and 11:18 a.m. on a specific day, cutting commenced from the position of JSD-D-07, encompassing all east-west monuments in Zone D. This was accompanied by chiseling and drilling beneath the monument on the westernmost side of Zone D. The sudden change in acceleration values during this period may be attributed to the vibration of the steel beam at the bottom of the monument due to the construction work at the site. The acceleration in the vertical direction of JSD-D-09 exceeds that in the vertical direction of JSD-D-07, presumed to be a result of cutting in the vicinity of the steel beam underneath the acceleration sensor JSD-D-09. The test results for JSD-D-01 to JSD-D-09 are detailed in table 11.

Conclusions

To enhance the seismic resilience of precious historical relics, a health monitoring system, combined with multi-source data analysis and intelligent algorithms, was employed to assess the impact of renovation projects and ensure the safety of these artifacts during construction. This research contributes to the field by designing an advanced structural health monitoring system tailored for large-scale artifacts, such as monuments, in the context of functional improvement. The system integrates multiple sensors, data acquisition systems, and management platforms to achieve automation, real-time monitoring, and network connectivity, thereby offering comprehensive surveillance of the relics' condition.

A key innovation of this study is the application of data fusion techniques to combine interrelated monitoring data, enabling more reliable assessments of the artifacts' structural health. Furthermore, intelligent algorithms were leveraged to automatically detect construction-related impacts, providing an efficient method

Table 11. Structural dynamic response analysis.

Serial number	Accelerating curve	Scene picture
JSD-D-01		
JSD-D-02		
JSD-D-03		
JSD-D-04		
JSD-D-05		
JSD-D-06		

Table 11. (Continued.)

Serial number	Accelerating curve	Scene picture
JSD-D-07		
JSD-D-08		
JSD-D-09		

for assessing the risks associated with ongoing work. In comparison to previous studies, this approach offers a more robust and data-driven framework for real-time structural monitoring, addressing challenges that have been inadequately explored in earlier literature. For example, many existing systems rely on manual evaluations and static data, whereas the integrated system in this research automates data processing and incorporates dynamic monitoring parameters, such as tilt, settlement, and crack width, significantly improving predictive capabilities.

The findings of this study highlight that the combination of automated monitoring and intelligent data processing can significantly enhance the resilience of historical artifacts during renovations. The real-time detection and early warning capabilities of the system are crucial for mitigating risks and ensuring the preservation of cultural heritage. However, while the system proved effective in the context of this project, further improvements could include the integration of passive and wireless sensors for cost-effectiveness and ease of deployment. Additionally, combining static and dynamic data from diverse sources would enhance the system's accuracy and contribute to more precise evaluations of the artifacts' health. Future work could explore these enhancements to further optimize the system's capabilities and improve its applicability to a broader range of cultural preservation projects.

Data availability statement

The data cannot be made publicly available upon publication because they contain sensitive personal information. The data that support the findings of this study are available upon reasonable request from the authors.

ORCID iDs

Songtao Xue  <https://orcid.org/0000-0002-6598-670X>

Qinhao Shi  <https://orcid.org/0009-0006-4155-0246>

Liyu Xie  <https://orcid.org/0000-0001-5777-0645>

References

- [1] Ožić K, Markić I, Moretić A and Lulić L 2023 The Assessment and Retrofitting of Cultural Heritage—a case study of a residential Building in Glina *Buildings* **13** 1798
- [2] Okpalanozie O E and Adetunji O S 2021 Architectural heritage conservation in nigeria: the need for innovative techniques *Heritage* **4** 2124–39
- [3] Aleksić J, Zečirović L, Dragović D, Slavković B, Suljević J and Božović J 2022 Seismic rehabilitation techniques for conserving and managing cultural heritage of old city fortress in novi pazar *Applied Sciences* **12** 12018
- [4] Zhang Q, Zhang Z and Chen X 2022 Influence of the deterioration type and age on the deterioration degree of 191 ancient limestone steles in the guihai forest of steles, Southern China *Environ. Earth Sci.* **81** 477
- [5] Zena A G 2023 Social and ritual practices behind the construction of stele monuments in gedee zone, South Ethiopia *J. of Archaeological Science: Reports* **47** 103767
- [6] Kaur P 2022 Legal regime for the protection of heritage stone monuments in india: a study with special reference to taj mahal and lotus temple *Geoheritage* **14** 87
- [7] Mammaeb M M 2022 Stele Of The 16th C. from kumukh village — a highly artistic work of islamic art *Proceedings in Archaeology and History of Ancient and Medieval Black Sea Region* **973–82**
- [8] Goded T, Irizarry J and Buform E 2012 Vulnerability and risk analysis of monuments in Málaga city's historical centre (Southern Spain) *Bull. Earthquake Eng.* **10** 839–61
- [9] Despotaki V, Silva V, Lagomarsino S, Pavlova I and Torres J 2018 Evaluation of seismic risk on UNESCO cultural heritage sites in Europe *International Journal of Architectural Heritage* **12** 1231–44
- [10] Davis C et al 2020 Identifying archaeological evidence of past earthquakes in a contemporary disaster scenario: case studies of damage, resilience and risk reduction from the 2015 gorkha earthquake and past seismic events within the kathmandu valley UNESCO world heritage property (Nepal) *J. Seismol* **24** 729–51
- [11] Protecting Cultural Heritage after the Earthquakes <https://news.un.org/en/story/2023/04/1135532>
- [12] Qiang Y and Chen G 2015 The engraving and value of the kaicheng stone classics of the tang dynasty *WENBO* **05**
- [13] Ning X, Dai J, Bai W, Yang Y and Zhang L 2018 Seismic protection of cabinet stored cultural relics with silicone dampers *Shock and Vibration* **2018** 1–15
- [14] Zou X, Yang W, Liu P and Wang M 2023 Shaking table tests and numerical study of a sliding isolation bearing for the seismic protection of museum artifacts *Journal of Building Engineering* **65** 105725
- [15] Chun Q, Meng Z and Hua Y 2018 Aseismic strengthening techniques of chinese typical stele relics: a case study of Xi'an Beilin *Journal of Southeast University* **34** (English Edition) 323–30
- [16] De Stefano A and Clemente P 2009 Structural health monitoring of historical structures *In Structural Health Monitoring of Civil Infrastructure Systems* (Elsevier) **412–34**
- [17] Baeza F J, Ivorra S, Bru D and Varona F B 2018 Structural health monitoring systems for smart heritage and infrastructures in Spain *Mechatronics for Cultural Heritage and Civil Engineering (Intelligent Systems, Control and Automation: Science and Engineering)* **92** ed E Ottaviano, A Pelliccio and V Gattulli (Springer International Publishing) **271–94**

- [18] Solís M, Romero A and Galvín P 2010 Monitoring the mechanical behavior of the weathervane sculpture mounted atop seville cathedral's giralda tower *Structural Health Monitoring* **9** 41–57
- [19] Saisi A, Gentile C and Ruccolo A 2018 Continuous monitoring of a challenging heritage tower in Monza, Italy *J Civil Struct Health Monit* **8** 77–90
- [20] Gentile C, Ruccolo A and Canali F 2019 Long-term monitoring for the condition-based structural maintenance of the milan cathedral *Constr. Build. Mater.* **228** 117101
- [21] De Stefano A, Matta E and Clemente P 2016 Structural health monitoring of historical heritage in italy: some relevant experiences *J Civil Struct Health Monit* **6** 83–106
- [22] Zhang R, Xie L and Lu W 2020 Translocation monitoring system for the mahavira hall of jade buddha temple(i): design and implementation *Struct Eng* **36** 196–203
- [23] Klein L, Bermudez S, Schrott A, Tsukada M, Dionisi-Vici P, Kargere L, Marianno F, Hamann H, López V and Leona M 2017 Wireless sensor platform for cultural heritage monitoring and modeling system *Sensors* **17** 1998
- [24] D'Alessandro A et al 2019 Urban seismic networks, structural health and cultural heritage monitoring: the national earthquakes observatory (INGV, Italy) experience *Front. Built Environ.* **5** 127
- [25] Chalkidou S, Arvanitis A, Patias P and Georgiadis C 2021 Spatially enabled web application for urban cultural heritage monitoring and metrics reporting for the SDGs *Sustainability* **13** 12289
- [26] Kullaa J 2010 Sensor validation using minimum mean square error estimation *Mech. Syst. Sig. Process.* **24** 1444–57
- [27] Jiang H, Wan C, Yang K, Ding Y and Xue S 2022 Continuous missing data imputation with incomplete dataset by generative adversarial networks–based unsupervised learning for long-term bridge health monitoring *Structural Health Monitoring* **21** 1093–109
- [28] Bloemhevel S, Van Den Hoogen J and Atzmueller M 2021 A computational framework for modeling complex sensor network data using graph signal processing and graph neural networks in structural health monitoring *Appl. Netw. Sci.* **6** 97
- [29] Wang Y W, Zhang C, Ni Y Q and Xu X Y 2022 Bayesian probabilistic assessment of occupant comfort of high-rise structures based on structural health monitoring data *Mech. Syst. Sig. Process.* **163** 108147
- [30] Tan X, Chen W, Zou T, Yang J and Du B 2023 Real-time prediction of mechanical behaviors of underwater shield tunnel structure using machine learning method based on structural health monitoring data *Journal of Rock Mechanics and Geotechnical Engineering* **15** 886–95
- [31] Ierimonti L, Venanzi I, Cavalagli N, García-Macías E and Ubertini F 2023 A bayesian-based data fusion methodology and its application for seismic structural health monitoring of the consoli palace in Gubbio, Italy *Procedia Structural Integrity* **44** 2082–9
- [32] Chen C, Tang L, Lu Y, Wang Y, Liu Z, Liu Y, Zhou L, Jiang Z and Yang B 2023 Reconstruction of long-term strain data for structural health monitoring with a hybrid deep-learning and autoregressive model considering thermal effects *Eng. Struct.* **285** 116063
- [33] Wang J, Liu H, Han Z and Wang Y 2023 Automatic identification method of bridge structure damage area based on digital image *Sci Rep.* **13** 12532
- [34] Lee I Y, Jang J and Park Y-B 2022 Advanced structural health monitoring in carbon fiber-reinforced plastic using real-time self-sensing data and convolutional neural network architectures *Mater. Des.* **224** 111348
- [35] Ni Y Q, Hua X G, Wong K Y and Ko J M 2007 Assessment of bridge expansion joints using long-term displacement and temperature measurement *J. Perform. Constr. Facil* **21** 143–51
- [36] Zhou G-D and Yi T-H 2013 The node arrangement methodology of wireless sensor networks for long-span bridge health monitoring *Int. J. Distrib. Sens. Netw.* **9** 865324
- [37] Wang G, Ding Y, Feng D and Ye J 2018 Evaluation of the wind-resistant performance of long-span cable-stayed bridge using the monitoring correlation between the static cross wind and its displacement response *Shock and Vibration* **2018** 1–10
- [38] Avci O, Abdeljaber O, Kiranyaz S, Hussein M and Inman D J 2018 Wireless and real-time structural damage detection: a novel decentralized method for wireless sensor networks *J. Sound Vib.* **424** 158–72
- [39] Li X, Xie L, Lu W, Xue S, Hong C, Lan W and Shi Q 2023 Structural health monitoring of a historic building during uplifting process: system design and data analysis *Structural Health Monitoring* **22** 3165–88
- [40] Pei H, Zhang F, Zhu H, Liu J, Ning F and Chen W 2023 Development of a distributed three-dimensional inclinometer based on OFDR technology and the frenet-serret equations *Measurement* **223** 113769
- [41] Chen S and Wang X 2021 Design of monitoring system for urban low-lying water *J. Phys. Conf. Ser.* **2029** 012128
- [42] Jeong S, Ferguson M, Hou R, Lynch J P, Sohn H and Law K H 2019 Sensor data reconstruction using bidirectional recurrent neural network with application to bridge monitoring *Adv. Eng. Inf.* **42** 100991
- [43] Oh B K, Park Y and Park H S 2020 Seismic response prediction method for building structures using convolutional neural network *Struct Control Health Monit* **27**
- [44] Lei X, Sun L and Xia Y 2021 Lost data reconstruction for structural health monitoring using deep convolutional generative adversarial networks *Structural Health Monitoring* **20** 2069–87
- [45] Chen J, Ding L, Ji J and Zhu J 2023 A combined method to build bayesian network for fire risk assessment of historical buildings *Fire Technol.* **59** 3525–63
- [46] Zhou Y, Luo X, Ye P, Zhang W, Qin L and Du Z 2023 Bayesian-based prediction and real-time updating of axial deformation in high-rise buildings during construction *Eng. Struct.* **297** 116992